ELSEVIER

Nuclear Physics B (Proc. Suppl.) 69/1–3 (1998) 286–293

NUCLEAR PHYSICS B
PROCEEDINGS
SUPPLEMENTS

High energy properties of X–ray sources observed with *BeppoSAX*

F. Frontera[a,b], D. Dal Fiume[b], G. Malaguti[b], L. Nicastro[b], M. Orlandini[b], E. Palazzi[b], E. Pian[b], F. Favata[c], A. Santangelo[d],

[a] Dipartimento di Fisica, Università di Ferrara, Via Paradiso 12, 44100 Ferrara, Italy

[b] Istituto Tecnologie e Studio Radiazioni Extraterrestri (TeSRE), C.N.R., via Gobetti 101, 40129 Bologna, Italy

[c] Astrophysics Division, Space Science Department of ESA, ESTEC Keplerlaan 1, 2200 AG Noordwijk, The Netherlands

[d] Istituto Fisica Cosmica e Applicazioni all'Informatica (IFCAI), C.N.R., via La Malfa 153, 90146 Palermo, Italy

We report on highlight results on celestial sources observed in the high energy band (> 20 keV) with *BeppoSAX*. In particular we review the spectral properties of sources that belong to different classes of objects, *i.e.*, stellar coronae (Algol), supernova remnants (Cas A), low mass X–ray binaries (Cygnus X–2 and the X–ray burster GS1826–238), black hole candidates (Cygnus X–1) and Active Galactic Nuclei (Mkn 3). We detect, for the first time, the broad-band spectrum of a stellar corona up to 100 keV; for Cas A we report upper limits to the ^{44}Ti line intensities that are lower than those available to date; for Cyg X–2 we report the evidence of a high energy component; we report a clear detection of a broad Fe K line feature from Cyg X–1 in soft state and during its transition to hard state; Mkn 3 is one of several Seyfert 2 galaxies detected with *BeppoSAX* at high energies, for which Compton scattering process is important.

1. INTRODUCTION

High energy properties of celestial X–ray sources give important information to understand their radiation mechanisms and the energetic processes occurring in them and/or in their environments.

Hard X–ray emission (> 20 keV) is currently observed from several classes of X–ray sources. Galactic X–ray sources that are known emitters of hard X–rays include black-hole candidates, X–ray pulsars, weak-magnetic-field neutron stars in Low Mass X–ray Binaries (LMXRBs), mainly X–ray bursters (XRBs), Cataclismic Variables (CV), in particular Polars, Crab-like supernova remnants.

High energy spectra of black-hole candidates (BHC) have permitted to infer the presence of Comptonization processes of soft photons occurring close to the black-hole (*e.g.*, in a disk corona).

XRBs, that are weakly magnetized neutron stars (with surface field intensity $B \leq 10^{10}$–10^{11} G), turned out to be hard X–ray emitters, once the sensitivity of the high energy instruments was increased at the 10 mCrab level (see [1] for a recent review). From their spectral properties, similarities with and diversities from BHCs have been inferred, like the presence of an accretion disk that can extend, as in the case of BHC, close to the surface of the compact object, and the presence of an additional component of soft photons that, unlike in BHCs, originates from the neutron star surface and can be a major source of thermal emission and electron cooling through Comptonization.

X–ray pulsars are well known emitters of hard X–rays. Observations in the hard X–ray band are relevant in order to get a measurement of the magnetic field intensity at the neutron star surface. Even if current models of the X–ray spectrum of these objects are still unsatisfactory at high energies, the measurement of cyclotron resonance features gives a direct estimate of the inten-

PII S0920-5632(98)00227-8

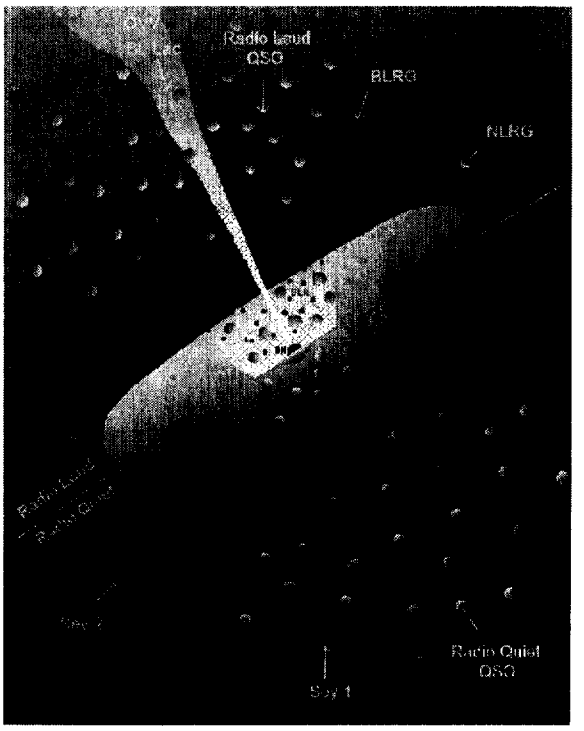

Figure 1. Unified model for AGNs. Adapted from [4].

sity of the neutron star magnetic field strength [2].

Emission from young shell-like supernova remnants mainly extends to low energies (< 20 keV). Detection of hard X–rays with determination of their spectral properties can provide important information on the emission mechanism (thermal vs. non thermal, like synchrotron radiation).

From stellar coronae, apart the Sun, hard X–rays have never been observed. As we will see, this gap has been filled with *BeppoSAX*.

Among the extragalactic X–ray sources, hard X–ray emission is observed from Active Galactic Nuclei (AGNs), that include Seyfert galaxies of both types (1 and 2), radio quiet QSOs and radio loud QSOs (which include blazars). A great effort is currently under way to interpret the different classes of AGNs in a unified scheme, which is sketched in Fig. 1. The basic energy production mechanism is accretion of matter onto a massive black hole ($\approx 10^8$ $M_\odot$) via an accretion disk. A massive toroid of larger radius (in the range from several parsecs to few tens of parsecs [3]) is assumed to surround the accretion disk. Depending on the configuration of the disk with respect to the toroid, on their relative sizes and distances, and on the viewing angle, an AGN should show different observational features and thus fall in one of the different classes above mentioned.

The above scheme is being tested also for stellar-mass black holes (*e.g.*, Cygnus X–1). Thus the unified scheme can be a general picture to interpret galactic and extragalactic black holes, accreting matter via an accretion disk. Given many similarities in the X–ray emission from stellar mass BHs with low-magnetic-field neutron stars in LMXRBs, the unified scheme now applied to AGNs could be extended to several classes of X–ray sources. Hard X–ray spectral properties of these sources can provide unique information to diagnose the presence of a black hole versus a weak-magnetic-field neutron star, to test the unified model for AGNs and its validity for stellar mass BHCs.

Thank to a broad energy band of operation (0.1–300 keV) and a uniform flux sensitivity in this range, *BeppoSAX* [5] has the unmatched capability of simultaneously sampling the spectrum of X–ray sources over more than three decades of energy.

The SAX/PDS instrument [6], with a sensitivity of about 1 mCrab at 100 keV, allows an accurate determination of the spectrum of many X–ray sources at the highest energies (13–200 keV).

For the brightest sources (> 10 mCrab), the HPGSPC instrument (6–60 keV) [7] provides the spectral coverage necessary to match the information provided by the low energy instruments LECS (0.1–10 keV) [8] and MECS (2–10 keV) [9] telescopes and the PDS.

Here we review some relevant results obtained with *BeppoSAX* during its Performance Verification Phase and first year Core Program, with particular focus on the PDS instrument. The spectral deconvolution was performed with the XSPEC software package, by using the instrument response function distributed from the *Bep-*

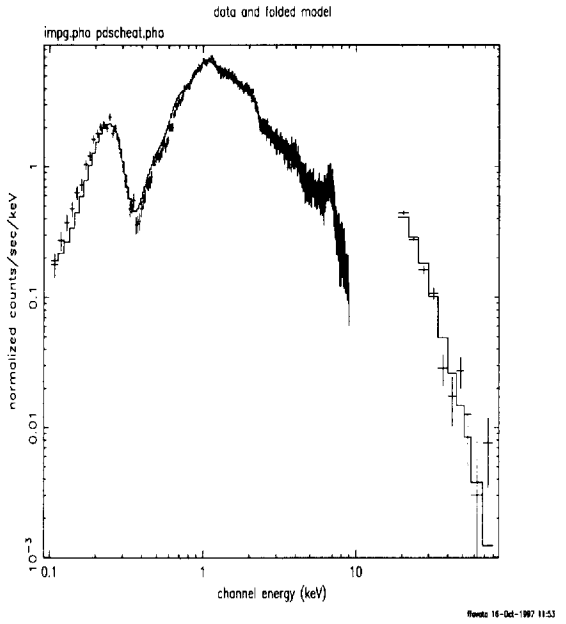

Figure 2. Count rate spectrum of Algol during the maximum of a long flare as observed by *BeppoSAX*. Superposed is the best fit thermal model [12].

poSAX Scientific Data Center.

2. HIGHLIGHT RESULTS

The reviewed sources span a large range of intensities and include a stellar corona (Algol), a supernova remnant (Cas A), two LMXRBs, one of which (Cygnus X–2) is a Z source and the other (GS1826–634) is an X–ray burster, a BHC (Cygnus X–1) observed in two different spectral states and the Seyfert 2 galaxy Mkn 3.

2.1. Algol

The general nature of stellar coronae as a class of thermal soft X–ray emitters was already established with the *Einstein* observatory [10]. The extensive observations with soft X–ray telescopes (*Einstein*, ROSAT) has shown that the typical peak plasma temperatures in the more active sources are of the order of a few keV, although during intense flares their X–ray luminosity and coronal temperatures increases strongly, leading to the expectation that hard X–rays may be detected. This phenomenon has been confirmed during the recent observation with *BeppoSAX* of Algol [11]. Algol is a binary system composed by a B8V and a K2IV star, with a binary period of 2.9 days. *BeppoSAX* observed the complete evolution of a large flare, lasting about 1 day. During the flare the soft (0.1–10 keV) X–ray luminosity increased by a factor more than 20. The source spectrum measured with LECS and PDS instruments during the peak of the flare is shown in Fig. 2. The flare spectrum is reasonably described with a two component emission model from a hot diffuse gas (MEKAL model in XSPEC) [12]. The preliminary analysis shows no evidence for the presence of a non-thermal component, up to highest observed energies. The characteristic temperatures of the flare spectrum are of the order of $\sim 2 \times 10^7$ and $\sim 1 \times 10^8$ °K. Further details of this observation are described in [11].

2.2. Cas A

The supernova remnant Cas A was observed with *BeppoSAX* on August 6, 1996. A non-thermal high-energy component in the X–ray emission from the source has been clearly detected [13]. The broad-band (0.5–100 keV) X–ray spectrum of the source (see Fig. 3) is modeled using the sum of three components: one Non-Equilibrium of Ionization (NEI) plasma component representing the emission from the ejecta; one NEI component representing the emission from the shocked material surrounding the circumstellar medium; a power law (PL) component to model hard X–ray emission. Best fit parameter values of the PL are a photon index of $2.95^{+0.10}_{-0.05}$ and a normalization parameter of 0.69 ph cm^{-2} s^{-1} keV^{-1} at 1 keV. The power law high energy component is very likely of synchrotron origin [14]. It gives a sizeable contribution at lower energies, being comparable in intensity to the thermal continuum at the position of the Fe K complex.

The search for radioactive emission lines due to ^{44}Ti formed during the supernova explosion

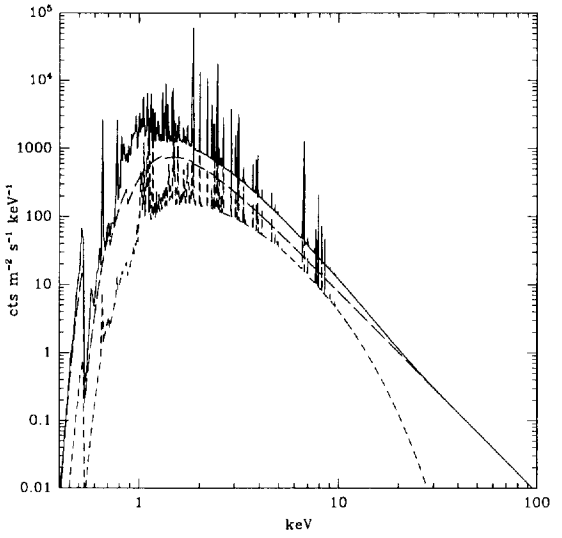

Figure 3. Deconvolved spectrum of Cas A. The different components are shown. From [13].

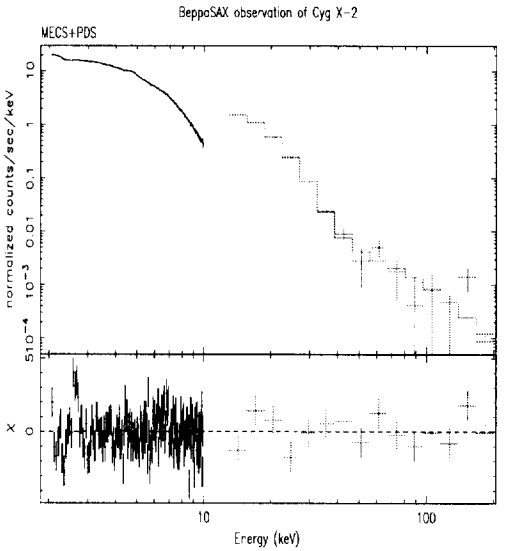

Figure 4. Top: 2–200 keV count rate spectrum of Cygnus X–2 with superposed the best fit model (see text). Bottom: residuals with respect to the model.

gives a 2σ upper limit to the intensity of the line at 68 keV of 1.3×10^{-5} ph cm^{-2} s^{-1} and an upper limit a factor about 10 times lower (4.4×10^{-6} ph cm^{-2} s^{-1}) at 78 keV. A 99% upper limit of 8.6×10^{-5} ph cm^{-2} s^{-1} for both lines was given by [15] with OSSE and a similar value was obtained with RXTE [16].

2.3. CYGNUS X–2

The LMXRB Cygnus X–2 is a member of a binary system (binary period of 9.84 days), consisting of a low-magnetic-field neutron star and a late type low-mass ($\sim 0.7\,M_\odot$) star V1341 Cyg [17–19]. It is classified as Z source, on the basis of its X–ray colour-colour spectral behaviour [20,21]. Its low-energy continuum spectrum, measured with the EXOSAT satellite, can be fitted with a Comptonization model ($kT = 3.7$ keV, optical depth $\tau = 9.4$) plus a black body component ($kT = 1.21$ keV) [22]. An emission Fe K line was first detected with the *Tenma* [23] and EXOSAT [24] satellites and, later on, it was resolved with the Broad Band X–ray Telescope (BBXRT) which detected a broad (FWHM = 0.97 keV) line with centroid energy 6.71 keV, and EW = 60 ± 27 eV [25].

Past high energy observations of Cygnus X–2 [26] showed that only a small fraction (about 1%) of the total source luminosity is emitted in hard X–rays.

BeppoSAX observed Cygnus X–2 on July 23, 1996, during the Science Verification Phase. Results obtained with the LECS instrument have been already published [27]. Here we report preliminary results of the same observation obtained with MECS and PDS. The on-source exposure times were about 40 ks for MECS and about 20 ks for PDS. Figure 4a shows the source spectrum in the 2–200 keV energy band. The broad-band spectrum is not well fit by the low-energy model described above (see Fig. 4b), yielding a reduced χ^2_ν of 1.62 for 179 degrees of freedom (dof). By

adding a power law component to fit the high energy excess χ^2_ν decreases to 1.51. The fit is still not satisfactory and thus a more suitable model has to be worked out, but this preliminary result shows that a high energy component is very likely present in the data. The preliminary model components and fit parameters are the following: soft blackbody with $kT_{bb} \simeq 1.5$ keV, Sunyaev and Titarchuk [28] Comptonization model with $kT_{ST} = 3.3$ keV and optical depth $\tau_{ST} \approx 9$ keV, high energy power law model with photon index $\alpha = 1.9 \pm 0.7$.

We estimated a possible contribution from the galactic ridge to the observed hard tail in the Cygnus X–2 spectrum. Using the results from Yamasaki et al. [29], we conclude that this contribution is a very small fraction of our 10–100 keV flux.

2.4. GS1826–238

GS1826–238 was discovered in September 1988 with *Ginga* [30] at a flux level of 26 mCrab in the 1–40 keV energy band with a hard power law spectrum (photon index $\Gamma = 1.7$). Later on, the source was detected at a 7σ significance level with OSSE above 50 keV with a steep power law spectrum ($\Gamma = 3.1 \pm 0.5$) [31]. The source was optically identified with a V19.3 star [32]. Given that its erratic flux time variability is reminiscent of that exhibited by Cygnus X–1, the source was classified by Tanaka and Lewin [33] as a black hole candidate. On March 31, 1997, the Wide Field Cameras (WFC) [34] aboard *BeppoSAX* detected three X–ray bursts from the source [35], suggesting that we are in presence of a weak magnetic field neutron star in a LMXRB.

BeppoSAX again observed the source on October 6–7, 17–18, and 27, 1997 as a target of opportunity (TOO). The first observation was triggered by a hard X–ray outburst with a peak flux of about 100 mCrab observed with the BATSE experiment aboard CGRO. We report here preliminary results obtained during the first observation. The exposure time was 7.7 ks for LECS, 21.7 ks for MECS and 10 ks for PDS. The 2–10 keV flux level from the source was 5.8×10^{-10} erg cm^{-2} s^{-1}, while at higher energies (20–100 keV) was 7.9×10^{-10} erg cm^{-2} s^{-1}.

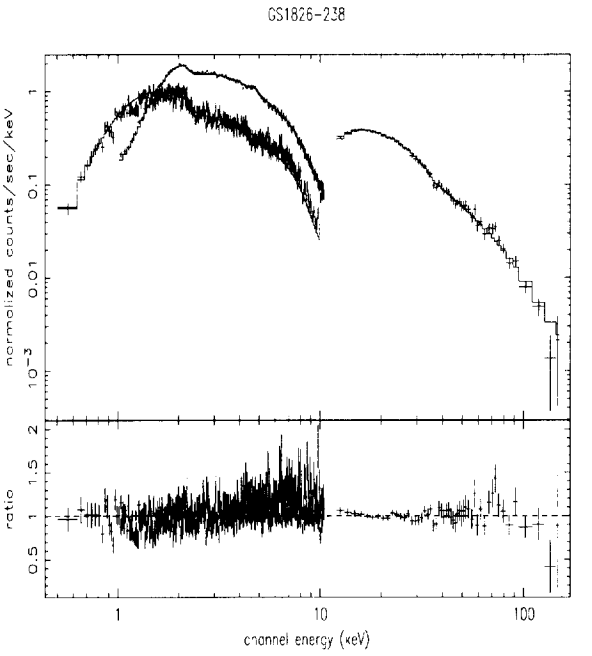

Figure 5. Top: Broad band count rate spectrum of GS1826–238 (1st TOO) with superposed the best fit model (see text). Bottom: residuals with respect to the model.

Figure 5 shows the broad-band count rate spectrum of the source. A best fit to the data is obtained with an absorbed blackbody (bb) plus a PL with an exponential cut-off. The best fit parameters are the following: $N_H = 5.1 \times 10^{21}$ cm^{-2}, $kT_{bb} \approx 1.21$ keV, PL photon index $\Gamma \approx 1.5$, high energy cut-off parameter approximately equal to 40 keV. X–ray bursts were observed during both the first and the second TOOs.

2.5. CYGNUS X–1

Cygnus X–1 is the most convincing example of a binary system that hides a stellar mass BH. As discussed above, AGNs are the best candidate objects to contain massive BH. The Compton reflection model used for AGNs is suggested to hold for Cygnus X–1 as well (see, *e.g.*, [36,37]). A test for the validity of this model for Cygnus X–1 is the presence of a broad Fe K emission line in the

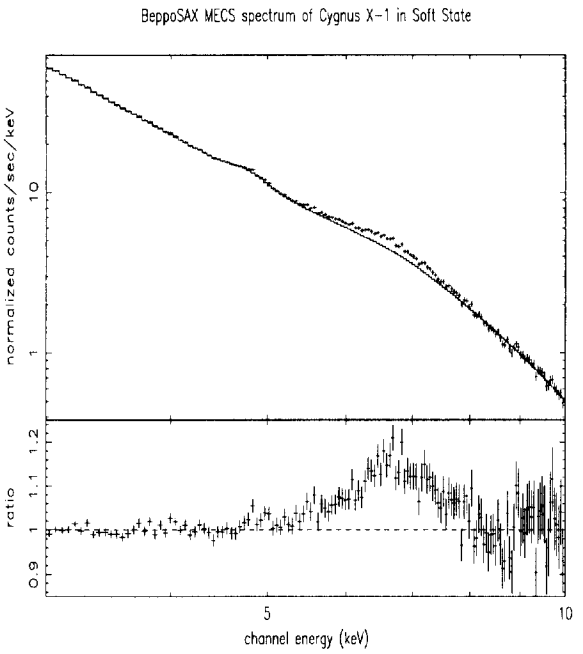

Figure 6. Top: Count rate spectrum of Cygnus X–1 measured by MECS during the June 25, 1996 observations. The other *BeppoSAX* instruments were switched off. Superposed is the best fit power law model to the continuum (excluded from the fit the 4.5–8.5 keV band). Bottom: excesses from the the model. The broad Fe K line is apparent with no clear evidence of a K edge.

X–ray spectrum of the source as a result of fluorescence from the disk. This line was actually detected with EXOSAT/GSPC [38] during a hard X–ray state of the source, but not confirmed in high resolution observations of Cygnus X–1 with the BBXRT [39] and ASCA [40] missions.

BeppoSAX observed the source three times during 1996, on June 22 and 25, during which the source was in soft state (SS) and on September 12, when the source was going back to its normal hard X–ray state (HS). Final results of these observations will be reported elsewhere [41]. Here we report preliminary results on the Fe K line feature. A broad line is observed in all the above observations. Figure 6 shows the count rate spectrum in the 2–10 keV band measured with the MECS telescopes during the 25 June observation. Only during the first SS observation a Fe K edge is clearly detected ($E_{edge} = 7.6$ keV, $\tau_{max} = 0.24$). A reflection component in the continuum spectrum is detected with the HPGSPC detector (8.5–60 keV) in both SS and HS. Using a reflection model for the MECS continuum spectrum around the Fe line, with the reflection parameters estimated from HPGSPC, one obtains for the spectral feature during the second SS observation a best fit with a disk-line model with rest energy at 6.4 keV ($\chi^2_\nu = 1.1$). In the other observations, a Gaussian line profile gives better fits, independently of the continuum used (power law with or without a reflection component). The equivalent width is highest in the first observation (about 1 keV) and lower ($\sim$ 300 eV) in the other observations, independently of the source state. These results, if interpreted in terms of a Fe K fluorescence from an accretion disk around a BH, require a different dimension of the emission region.

2.6. Mkn 3

Mkn 3 ($z = 0.0135$) is a type 2 Seyfert first detected in X–rays by Ginga [42]. It was only marginally detected above 50 keV with the OSSE experiment aboard the *Compton* Gamma Ray Observatory [43].

It was observed with *BeppoSAX* on November 26, 1996. More details of this observation and results can be found elsewhere [44]. The flux level measured in the low (2–10 keV) energy band is 6×10^{-12} erg cm^{-2} s^{-1}, corresponding to 0.28 mCrab, while that in the high (20–100 keV) band is 1.3×10^{-10} erg cm^{-2} s^{-1}, corresponding to 7.6 mCrab, with a ratio (High/Low) = 27. The high energy spectrum has been determined up to 200 keV. Figure 7 shows the count rate spectrum of the source in the 0.6-200 keV energy band. Preliminary results indicate the presence of a soft excess, a prominent Iron Kα complex and a 15–50 keV hump. The heavily ($N_H \approx 10^{24}$ cm^{-2}) absorbed primary ionization provides only a few percent of the 2–10 keV flux, while it dominates above 10 keV, in the PDS band. This result can be interpreted in terms of the unified model of

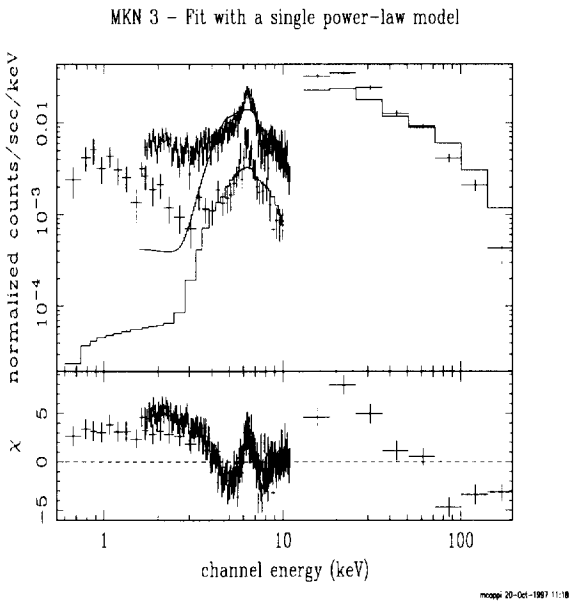

Figure 7. *BeppoSAX* spectrum of Mkn 3 fitted with an absorbed power law. The residuals indicate a strong Fe K line plus a 15–50 keV hump.

AGN [44].

3. CONCLUSIONS

Observations of celestial sources with *BeppoSAX* show new key results on their high energy (> 20 keV) spectral properties.

Strong high energy emission has been detected from Algol during 1 day long flare. The emission appears to be the tail of the thermal X–ray radiation.

LMXRBs are known sources of low energy X–ray emission, but the high energy emission is well known only for a small part of them (see a recent review by [1]). We detected for the first time a non thermal high energy component from the Z source Cygnus X–2 and derived, for the first time with the same satellite, the broad–band (0.1–200 keV) photon spectrum of an X–ray burster during a transient hard X–ray outburst. We expect to be able, using the three observations available, to study the relative behaviour of the high energy components with respect to the low-energy one as a function of the high energy flux of GS1826–238.

We have reported the clear detection of a broad Fe K line feature from Cygnus X–1 during a soft state of the source and we have discussed its behaviour for different spectral states. The Fe fluorescence emission does not appear to be consistent with a constant disk emission region.

As far as the AGNs are concerned, the detection of power laws with strong absorptions at lower energies and reflection components, is now observed for several Seyfert 2 galaxies. We have shown the outstanding example of Mkn 3.

REFERENCES

1. M. Tavani and D. Barret, to appear in Proc. 4th *Compton* Gamma-Ray Observatory Symposium, eds. J. Kurfess and R. Dermer, AIP Conf. Proc Series (1998), in press.
2. D. Dal Fiume et al., these proceedings.
3. J.H. Krolik, P. Madau, and P.T. Zycky, ApJ 420 (1994) L57.
4. C.M. Urry and P. Padovani, PASP 107 (1995) 803.
5. G. Boella et al., A&AS 122 (1997) 299.
6. F. Frontera et al., A&AS 122 (1997) 357.
7. G. Manzo et al., A&AS 122 (1997) 341.
8. A.N. Parmar et al., A&AS 122 (1997) 309
9. G. Boella et al., A&AS 122 (1997) 327.
10. G. Vaiana., J. Cassinelli, G. Fabbiano et al., ApJ 244 (1981) 163.
11. F. Favata, these proceedings.
12. R. Mewe, J. S. Kaastra, D. A. Liedahl, Legacy 6 (1995) 16.
13. F. Favata et al., A&A 324 (1997) L49.
14. G.E. Allen et al., ApJL 487 (1997) L97.
15. L.S The et al., ApJ 444 (1995) 244.
16. R.E. Rothschild et al., to appear in Proc. 4th *Compton* Gamma-Ray Observatory Symposium, eds. J. Kurfess and R. Dermer, AIP Conf. Proc Series (1998), in press.
17. A.P. Cowley, D. Crampton, and J.B. Hutchings, ApJ 231 (1979) 539.
18. J.E. McClintock et al., ApJ 282 (1984) 794.

19. S.M. Kahn and J.E. Grindlay, ApJ 281 (1984) 826.
20. N.S. Schulz, G. Hasinger and J. Trümper, A&A 225 (1989) 48.
21. R.A.D. Wijnands et al., A&A 323 (1997) 399.
22. N.E. White, L. Stella and A.N. Parmar, ApJ 324 (1988) 363.
23. T. Hirano et al., PASAJ 36 (1987) 619.
24. L. Chiappetti et al., ApJ 361 (1990) 596.
25. A.P. Smale et al., ApJ 410 (1993) 796.
26. G. Matt et al., ApJ 355 (1990) 468.
27. E. Kuulkers et al., A&A 323 (1997) 29L.
28. R.A Sunyaev and L.G. Titarchuk, A&A 201 (1980) 379.
29. Y. Yamasaki et al., ApJ 481 (1997) 821.
30. F. Makino, IAU Circ. No. 4653 (1988).
31. M. Strickman et al., A&AS 120 (1996) 217.
32. D. Barret, C. Motch and W. Pietsch, A&A 303 (1995) 526.
33. Y. Tanaka and W.H.G. Lewin in W.G.H. Lewin, J. van Paradijs and E.P.J. van den Heuvel (eds.), X-ray Binaries, Cambridge University Press, Cambridge, 1995, p.126.
34. R. Jager et al., A&AS (1998) in press.
35. P. Ubertini et al., IAU Circ. 6611 (1997).
36. C. Done, J.S. Mulchaey, K.A. Arnaud, ApJ 395 (1992) 275.
37. F. Haardt, C. Done, G. Matt and A.C. Fabian, ApJL 411 (1993) L95.
38. P. Barr, N.E. White and C.G. Page, MNRAS 216 (1987) 65P.
39. F.A. Marshall, R.F. Mushotzky, R. Petre, and P.J. Serlemitsos, ApJ 419 (1993) 301.
40. K. Ebisawa et al., ApJ 467 (1996) 419.
41. F. Frontera et al., in preparation (1998).
42. H. Awaki et al., Nature 346 (1990) 544.
43. W.N. Johnson, private communication (1997).
44. G. Malaguti et al., these proceedings.